IEEE Photonics Journal
An IEEE Photonics Society Publication

Open Access

Experimental Analysis of the Power Auto-Correlation-Based Chromatic Dispersion Estimation Method

Volume 5, Number 4, August 2013

Fernando C. Pereira
Valery N. Rozental
Marco Camera
Gianmarco Bruno
Darli A. A. Mello

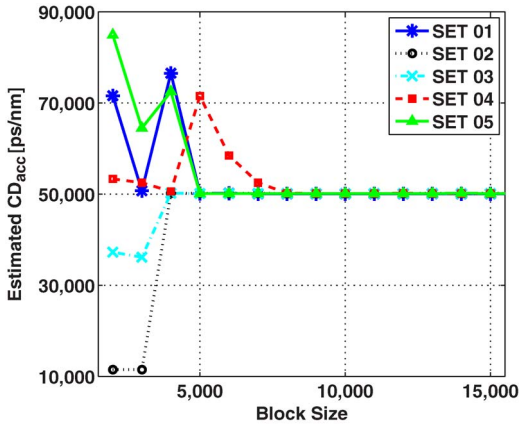

DOI: 10.1109/JPHOT.2013.2272782
1943-0655/$31.00 ©2013 IEEE

IEEE photonics SOCIETY

IEEE

Experimental Analysis of the Power Auto-Correlation-Based Chromatic Dispersion Estimation Method

Fernando C. Pereira,[1] Valery N. Rozental,[1] Marco Camera,[2] Gianmarco Bruno,[2] and Darli A. A. Mello[1]

[1]OCNLab, Department of Electrical Engineering, University of Brasilia, 70910-900 Brasília-DF, Brazil
[2]Ericsson Telecomunicazioni, 16153 Genova, Italy

DOI: 10.1109/JPHOT.2013.2272782
1943-0655/$31.00 ©2013 IEEE

Manuscript received June 12, 2013; revised July 2, 2013; accepted July 5, 2013. Date of publication July 11, 2013; date of current version July 17, 2013. This work was supported by the Innovation Center, Ericsson Telecomunicaçoes S.A., Brazil. Corresponding author: V. N. Rozental (e-mail: valery@unb.br).

Abstract: We experimentally investigate the performance of the signal power auto-correlation-based method for chromatic dispersion (CD) estimation in a polarization-multiplexing quadrature phase-shift keying (PM-QPSK) 100G coherent optical system conveying optical channel transport unit level-4 (OTU4) frames. It is shown that the typical laboratory setup, where the signal components are generated from delayed versions of the same pseudorandom binary sequence (PRBS), is inadequate for experimental validation because of artifacts in the signal auto-correlation function. This problem is circumvented by the use of a commercial line card transporting independent data sequences. The algorithm is used to estimate accumulated CD values from 0 to 50 000 ps/nm under up to 80-ps differential group delay (DGD). We further evaluate its convergence properties in terms of the length of the sample vector required for correct CD estimation and address the hardware resource requirements. The CD-shifted version of the algorithm yielded a maximum estimation error of 186 ps/nm in all tested conditions.

Index Terms: Fiber optics, optical communications, chromatic dispersion estimation.

1. Introduction

In modern coherent optical systems, chromatic dispersion (CD) is compensated for in the digital domain [1], avoiding the use of optical dispersion compensation modules (DCMs). There are two main reasons for this choice: first, from the management perspective, it is more effective to replace dozens of DCMs, based on dispersion-compensating fibers or fiber Bragg gratings, by a digital signal processing (DSP) algorithm integrated to the receiver; second, DCMs lower the system signal-to-noise ratio because of their insertion loss. In addition, tolerance to nonlinearities is increased in dispersion unmanaged systems due to the walk-off phenomenon and phase decorrelation of the mixing signals. In order to be deployed in a flexible manner, future coherent transceivers should be seamlessly integrated into links of different lengths and fiber types. Moreover, in a scenario where new uncompensated link spans are deployed within the existing dispersion managed infrastructure, accumulated CD ceases to be a function of distance. Together with the ITU-T 50 ms system recovery time requirements [2], these considerations drive the need for accurate and fast CD estimation.

Several recent works have proposed to blindly estimate CD in the digital domain by scanning over a range of preset dispersion values, minimizing a certain cost function. Kuschnerov *et al.*, in [3], proposed a scanning time-domain estimation with constant modulus algorithm-based cost function.

In [4] a frequency-domain scanning algorithm with a modified discrete circular auto-correlation-based cost function was proposed. A different scanning algorithm proposed in [5] explored the relationship between the signal peak-to-average power ratio and the accumulated CD. Two timing error detector-based scanning algorithms were proposed in [6] and [7]. The algorithm in [6] uses a feed-forward detector. It is insensitive to transmission impairments and requires only few hardware resources. Its performance was not yet experimentally verified. The algorithm in [7], on the other hand, relies on the time error variance, and was experimentally validated for PM-QPSK and PM-16QAM transmission. Also, experimental implementation of several scanning algorithms based on different error metrics, namely, constant modulus algorithm, mean signal power, eigen-value spread and frequency spectrum auto-correlation, was performed in [8]. In general, scan-based algorithms must reduce the scanning step-size for more accurate estimation, increasing computational complexity (in terms of number of the required operations) and system start-up time. In [9], [10] a Godard clock-tone based, computationally efficient algorithm was presented, performing the best value scan by fast Fourier transform (FFT). However, clock-tone may be severely affected by polarization mode dispersion (PMD).

Sui *et al.*, in [11], [12], proposed a single-step estimation algorithm (auto-correlation signal power waveform–ACSPW) that uses the signal power auto-correlation. It was shown that there exists a mathematical dependency between the time delay that corresponds to the maximum value of the signal power auto-correlation function and accumulated CD. Therefore, unlike in the scanning algorithms, ACSPW performs CD estimation in a single step, allowing to reduce the system start-up time. In addition, Sui *et al.* analytically demonstrated robustness against amplified spontaneous emission (ASE) noise, differential group delay (DGD), frequency offset and laser phase noise [12]. Still, ACSPW yields incorrect results for small CD values. We overcame this problem in [13] by artificially introducing a known amount of CD using the bulk receiver equalizer, and subtracting this value after CD is estimated.

In this paper we present an experimental investigation of ACSPW with its aforementioned modification (further referred as CD-shifted ACSPW) for noisy transmission under CD and first-order PMD. We also assess the algorithm convergence properties in terms of the length of the sample vector required for accurate CD estimation, and discuss its hardware resource requirements. The rest of the paper is structured as follows: Section 2 reviews ACSPW and CD-shifted ACSPW; Section 3 describes the experimental setup; Section 4 presents the obtained results; and Section 5 concludes the paper.

2. CD Estimation Techniques

2.1. Auto-Correlation of the Signal Power Waveform Algorithm

Let $y[n] = |s[n]|^2$ be the instant power of the received signal $s[n]$. The auto-correlation function of $y[n]$, $\bar{R}_{yy}(\tau)$, can be separated into two components: $\bar{R}_{y_0y_0}(\tau)$, the component related to the power of individual symbols, and $\bar{R}_{y_1y_1}(\tau)$, the component related to the interference between symbols [11]. For a sufficiently high accumulated CD, the first term approaches a constant and the second term yields a peak value, whose position, τ_0, assuming Gaussian pulses, is related to the accumulated CD by [11]:

$$\arg\max_{\tau}\left\{\bar{R}_{y_1y_1}(\tau)\right\} = \tau_0 = \frac{2\pi\left(T_0^4 + \beta_2^2 z^2\right)}{T\beta_2 z}. \tag{1}$$

In Eq. (1) T is the symbol period, T_0 is the Gaussian pulse half-width at the $1/e$ point, z is the fiber length and β_2 is the group-velocity dispersion parameter. Next, the accumulated CD can be estimated from Eq. (1) by:

$$CD_{acc} = \beta_2 z \frac{2\pi c}{\lambda^2} = \frac{\tau_0 T + \sqrt{\tau_0^2 T^2 - 16\pi^2 T_0^4}}{4\pi} \frac{2\pi c}{\lambda^2}, \tag{2}$$

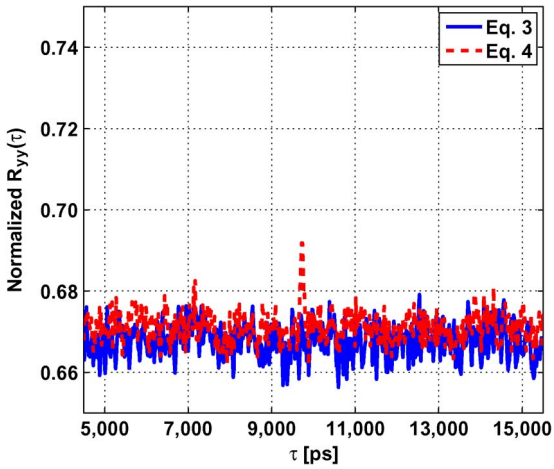

Fig. 1. Unfiltered and high-pass filtered auto-correlation function.

where c is the speed of light and λ is the carrier wavelength. Note that, after analog-to-digital conversion, the sample cross-correlation function of $y[n]$ can be efficiently calculated by:

$$\bar{R}_{yy}[n] = \text{IFFT}\Big\{|\text{FFT}(y[n])|^2\Big\}, \tag{3}$$

following the Wiener-Khintchine Theorem [14].

To further enhance the auto-correlation peak that otherwise may be too weak, a high-pass filter should be used [12]:

$$\bar{R}_{yy}[n] = \text{IFFT}\left\{\left|\text{FFT}\Big\{|s[n]-s[n+1]|^2\Big\}\right|^2\right\}. \tag{4}$$

To exemplify the high-pass filter enhancement, Fig. 1 depicts the normalized signal power auto-correlation function obtained from experimental data by Eq. (3) (unfiltered) and Eq. (4) (high-pass filtered) for OSNR $= 16$ dB, DGD $= 50$ ps and accumulated CD $= 40,000$ ps/nm. Clearly, high-pass filtering enhances the CD-related correlation peak (around 10,000 ps).

In systems with polarization multiplexing, the FFT argument in Eq. (4) becomes

$$|s_v[n]-s_v[n+1]|^2+|s_h[n]-s_h[n+1]|^2, \tag{5}$$

where subscripts v and h indicate the vertical and horizontal polarization orientations. It is important to note that, although Eq. (1) assumes Gaussian pulses, remarkably, the method is not limited to RZ pulse format. In particular, this experimental validation was performed with NRZ signal.

A main criticism of ACSPW is that it would require considerable hardware resources, namely, for the FFT/IFFT operations [6], because the FFT block for CD estimation is much larger than the FFT block for CD compensation. It is important to note, however, that the FFT/IFFT operations can still be handled by the dispersion compensation filter hardware. In non-dispersion-managed links, optical transceivers are typically dimensioned to compensate for up to 50,000 ps/nm of accumulated CD, which can be accomplished by a 1024-tap filter (for each polarization) with very little penalty [1]. For aliasing-free processing, this requires two 2048-coefficient FFT blocks. As for CD estimation, in Section 4 we show that 8000 signal samples are sufficient to compute the auto-correlation. Thus, Eq. (4) can be computed using a single 8192-coefficient FFT. But this FFT can be easily implemented by the decimation-in-time technique [15] with the aforementioned two 2048-coefficient FFT blocks and only minor additional storage requirements.

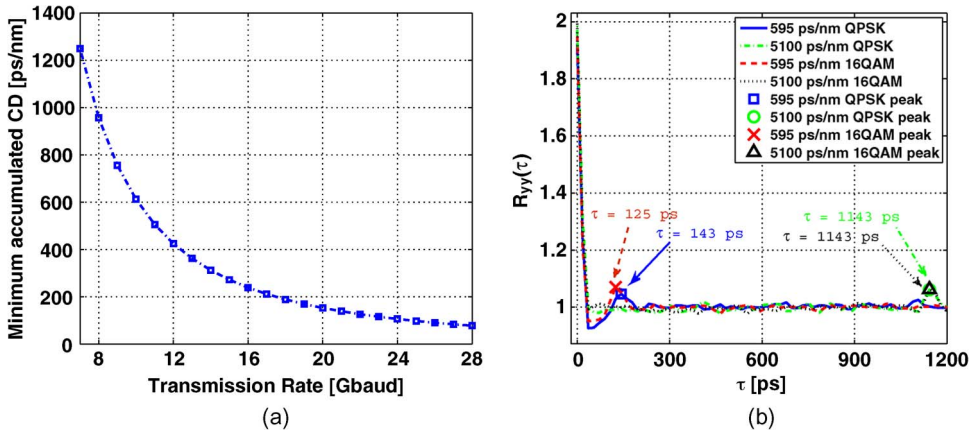

Fig. 2. (a) Minimal required accumulated CD *versus* transmission rate; and (b) auto-correlation for the CD values of 595 and 5100 ps/nm, obtained by simulation.

2.2. CD-Shifted ACSPW

For small accumulated CD values, the CD-associated auto-correlation peak vanishes. From inspection of Eq. (2) it follows that the argument of the square root must be positive to give real-valued CD estimates. Isolating τ_0 and finding the minimal value that yields a positive square-root argument, τ_{min}, we obtain [13]:

$$\tau_{min} = \frac{4 \cdot \pi \cdot T_0^2}{T}. \tag{6}$$

Replacing τ_{min} in Eq. (2), the theoretical minimum required accumulated CD is given by:

$$CD_{acc-min} = \frac{\tau_{min} T + \sqrt{\tau_{min}^2 T^2 - 16\pi^2 T_0^4}}{4\pi} \frac{2\pi c}{\lambda^2} = T_0^2 \frac{2\pi c}{\lambda^2}. \tag{7}$$

Note that $CD_{acc-min}$ depends on T_0. Fig. 2(a) shows the minimal accumulated CD as function of $1/T$, for $T_0 = 0.28T$ [11]. In addition, Fig. 2(b) shows the auto-correlation function for CD values of 595 and 5100 ps/nm, for 28 Gbaud QPSK and 16QAM simulated signals. The peaks appear in 143 and 1143 ps for QPSK, and 125 and 1143 ps for 16QAM. Introducing these values as τ_0 in Eq. (2) results in the estimated accumulated CD of 625 and 5073 ps/nm for QPSK, and 544 and 5073 ps/nm for 16QAM. That is, ACSPW can be successfully employed with both modulation formats.

For accumulated CD smaller than the required minimum, ACSPW returns a random value which may result in an estimation error of thousands of ps/nm. CD-shifted ACSPW overcomes this limitation by artificially adding a known CD quantity to the signal using a finite impulse response filter, to guarantee that the accumulated CD value is higher than the required minimum. After estimation, the added CD is subtracted from the estimated value.

3. Experimental Setup

Fig. 3 depicts the experimental setup. The transmitted polarization-multiplexing quadrature phase-shift keying (PM-QPSK) NRZ signal is generated by a 100G line card that creates optical channel transport unit level 4 (OTU4) frames [16] with soft-decision forward error correction (SD-FEC), at 120.576 Gb/s (30.144 Gbaud). In this way, the four signal components (in-phase (I) and quadrature (Q) components for orthogonal polarizations V_{pol}. and H_{pol}.) are uncorrelated. After being amplified for transmission, the signal passes through a CD generation module, composed by five cascaded fiber Bragg grating DCMs, each generating 10,000 ps/nm of CD. The generated dispersion is

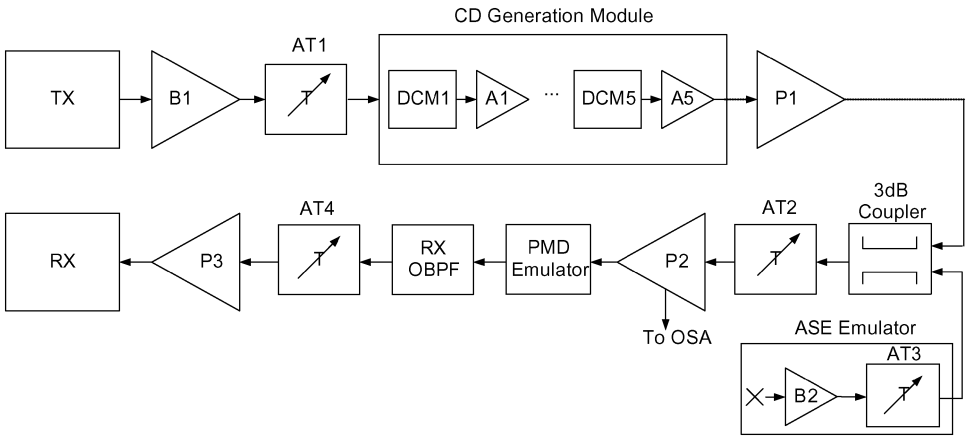

Fig. 3. Experimental setup. (Tx: transmitter; Rx: receiver; B1-2: optical booster amplifiers; P1-3: optical pre-amplifiers; AT1-4: variable optical attenuators; A1-5: optical amplifiers within the CD generation module; OSA: optical spectrum analyzer; OBPF: optical band-pass filter).

controlled by activating the DCMs selectively. Inside the CD generation module, cascaded optical amplifiers compensate for the DCM insertion loss. The amplified spontaneous emission (ASE) noise is generated by an optical amplifier and loaded into the signal by a 3-dB coupler. The optical signal-to-noise ratio (OSNR) is controlled by an optical attenuator (AT3). A PMD emulator introduces differential group delay (DGD), and performs arbitrary polarization scrambling. The polarization diversity coherent receiver, containing four pairs of balanced photodetectors, converts the optical field into the electric domain base-band signal. The four electrical outputs are sampled at 50 GSamples/s by a 4-channel oscilloscope (8-bits nominal resolution) and stored for offline post-processing. In total, five different polarization scrambled data sets were acquired for each of the transmission conditions studied in Section 4.

Observe that the algorithm parameters impose an intrinsic accuracy constraint on the algorithm due to the discrete nature of the delay τ_0. In the present setup, the time difference between subsequent samples (after resampling for two samples per symbol), and hence, the τ_0 temporal resolution, is 16.587 ps, According to Eq. (2), this resolution yields a precision of 69 ps/nm in CD estimation. From Eq. (2) it further follows that the precision-associated error is reduced with the symbol rate, provided that the sampling ratio of two samples per symbol is maintained.

A critical feature of ACPSW is that it relies on the complete decorrelation between the four electrical data flows. If decorrelation between the I-Q and the V-H_{pol}. signal components is obtained by delaying a particular PRBS–which is a common practice in experimental setups–non CD-related peaks appear on the power auto-correlation function, making the setup inadequate for experimental validation. To illustrate that, Fig. 4 shows the power auto-correlation function for a simulated PM-QPSK signal generated by four independent pseudo-random computer-generated data streams (Fig. 4(a)), and a second signal generated by a pseudorandom binary sequence (PRBS) of 2^{11} bits, where the I-Q and the V-H_{pol}. decorrelation is obtained by a 50 and a 1,050 symbols delay, respectively (Fig. 4(b)). While for the random data in Fig. 4(a) only one peak is observed, the use of the same PRBS decorrelated in time to generate the four modulator inputs in Fig. 4(b) results in spurious peaks, strongly degrading the estimation process.

4. Experimental Results

We start by evaluating the data block size required to estimate accumulated dispersion. The number of samples used to calculate the auto-correlation function, using Eq. (4), was varied from 1,000 to 15,000 $T/2$-spaced samples. Fig. 5 shows the results for selected accumulated CD values. The accumulated CD was correctly estimated for all data sets using 8,000 samples.

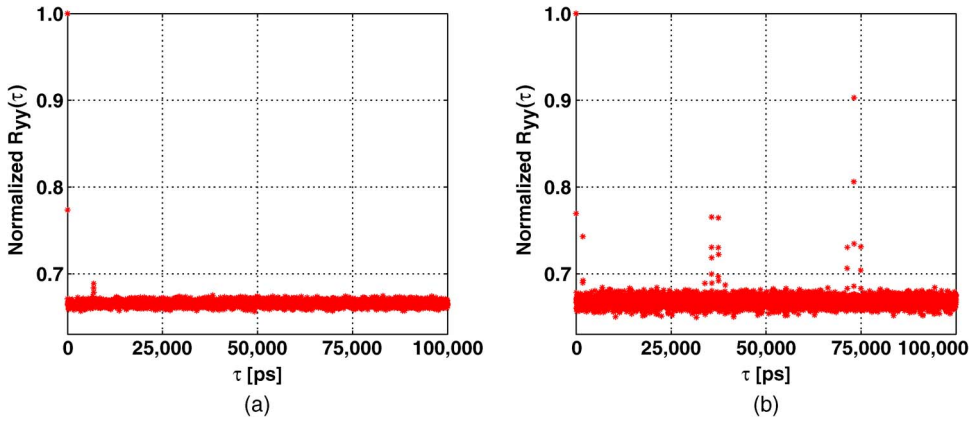

Fig. 4. Simulated auto-correlation function for a PM-QPSK signal generated by independent and delay-based decorrelated data streams. (a) Auto-correlation for four independent pseudo-random sequences. (b) Auto-correlation for a transmitted signal generated by time-shifted versions of the PRBS of 2^{11}.

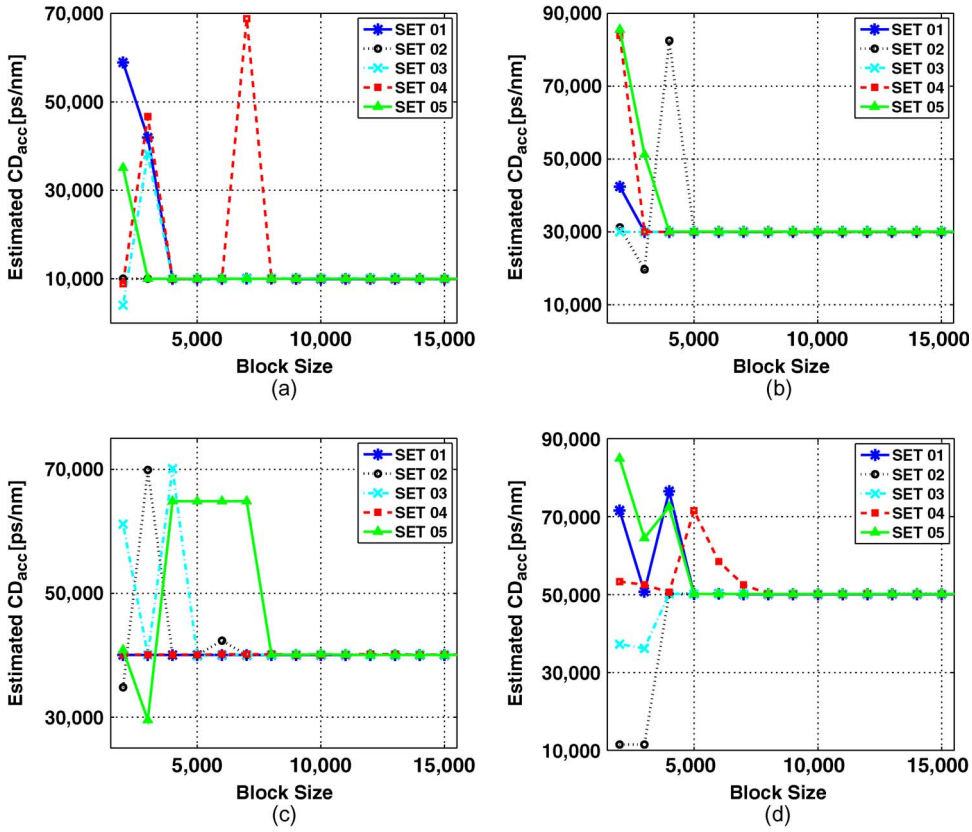

Fig. 5. Estimated accumulated CD *versus* number of samples for $\bar{R}_{yy}$ calculation. (a) Acc. CD $= 10,000$ ps/nm. (b) Acc. CD $= 30,000$ ps/nm. (c) Acc. CD $= 40,000$ ps/nm. (d) Acc. CD $= 50,000$ ps/nm.

Fig. 6(a) shows the estimates produced by ACSPW (blue squares) and CD-shifted ACSPW (red dots) for accumulated CD values from 0 to 50,000 ps/nm (a common range for these systems), for five different data sets of 10,000 samples. For accumulated CD values over 10,000 ps/nm, both

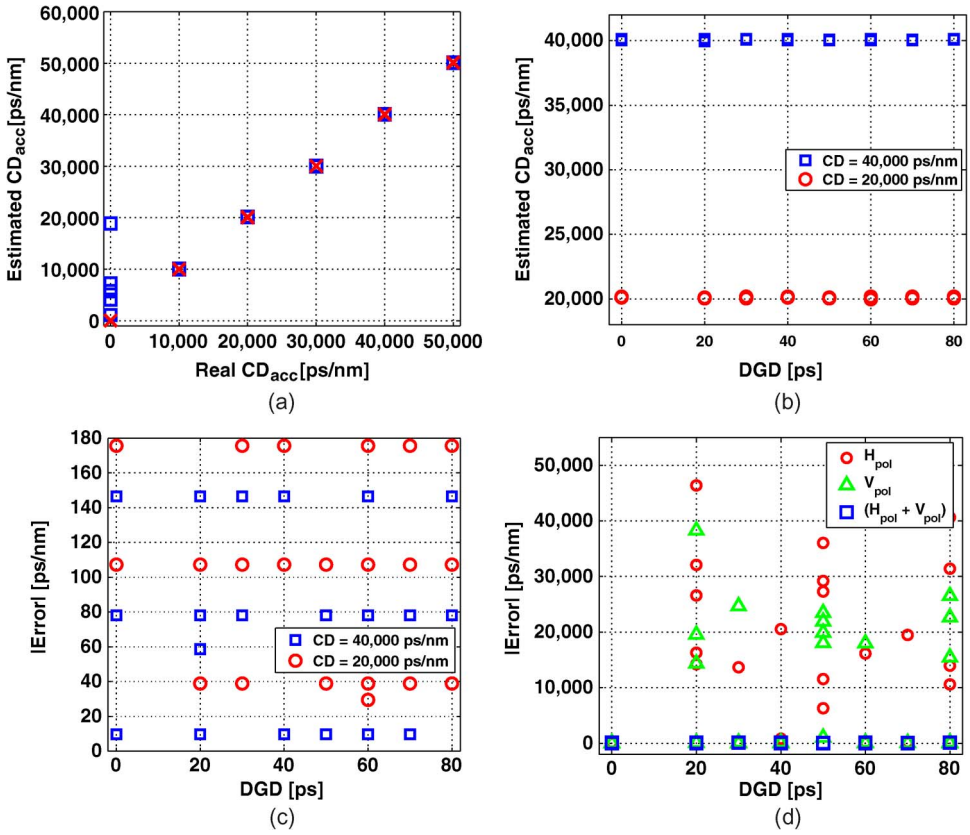

Fig. 6. Experimental results. (a) Estimated CD for ACPSW and CD-shifted ACSPW. (b) Effect of first-order PMD on the CD estimation. (c) Absolute error for different DGD values. (d) CD estimation for individual polarizations.

TABLE 1

Maximum estimation error for ACSPW and CD-shifted ACSPW

Acc. CD [ps/nm]	ACSPW [ps/nm]	CD-shifted ACSPW [ps/nm]
0	18,876	53
10,000	122	39
20,000	176	161
30,000	93	78
40,000	147	132
50,000	132	186

algorithms produced precise estimates with a maximum error of 176 and 186 ps/nm respectively (for all maximum error values, see Table 1). In the absence of CD, ACSPW produced arbitrary estimates, as expected, ranging from 1,000 to 20,000 ps/nm.

Fig. 6(b) presents the estimates for CD values of 20,000 and 40,000 ps/nm, when DGD is varied from 0 to 80 ps. The ACSPW exhibited a remarkable first-order PMD tolerance, suggesting that DGD has no effect on the performance of the algorithm, as it was theoretically predicted in [12]. Fig. 6(c) shows a high resolution absolute error value for the same data.

Finally, we estimated the accumulated CD analyzing individually signal components in V_{pol} (green triangles) and H_{pol} (red circles), comparing the results to the joint estimation, where signal power in both polarizations are added, as in Eq. (5). The results are shown in Fig. 6(d). Clearly,

power auto-correlation of the separate polarizations is severely affected by DGD, making the individual analysis infeasible.

5. Conclusion

We experimentally investigated the performance of the signal power auto-correlation based CD estimation algorithm in a PM-QPSK 100G system conveying OTU4 frames with SD-FEC. The need to use independent data streams to drive the modulator, instead of the time-decorrelated PRBSs typically used in laboratory experiments, was demonstrated. The algorithm required less than 10,000 $T/2$-spaced samples to converge in all investigated scenarios. Accumulated chromatic dispersion values up to 50,000 ps/nm were estimated with a maximum error of 186 ps/nm under first-order PMD of up to 80 ps. Also, our analysis showed that the algorithm requires very little additional hardware.

References

[1] S. J. Savory, "Digital filters for coherent optical receivers," *Opt. Exp.*, vol. 16, no. 2, pp. 804–8017, Jan. 2008.
[2] ITU-T Recommendation G.841: Types and Characteristics of SDH Network Protection Architectures, 1998. [Online]. Available: http://www.itu.int/rec/T-REC-G.841-199810-I/en
[3] M. Kuschnerov, F. N. Hauske, K. Piyawanno, B. Spinnler, A. Napoli, and B. Lankl, "Adaptive chromatic dispersion equalization for non-dispersion managed coherent systems," presented at the Optical Fiber Communication Conf., San Diego, CA, USA, Mar. 22–26, 2009, Paper OMT1.
[4] F. N. Hauske, C. Xie, Z. Zhang, C. Li, L. Li, and Q. Xiong, "Frequency domain chromatic dispersion estimation," presented at the Nat. Fiber Optic Engineers Conf., San Diego, CA, USA, Mar. 21–25, 2010, Paper JThA11.
[5] C. Xie, "Chromatic dispersion estimation for single-carrier coherent optical communications," *IEEE Photon. Technol. Lett.*, vol. 25, no. 10, pp. 992–995, May 2013.
[6] D. Wang, C. Lu, A. Lau, P. Wai, and S. He, "Adaptive CD estimation for coherent optical receivers based on timing error detection," *IEEE Photon. Technol. Lett.*, vol. 25, no. 10, pp. 985–988, May 2013.
[7] J. C. Diniz, S. Ranzini, V. Ribeiro, E. Magalhães, E. Rosa, V. Parahyba, L. V. Franz, E. E. Ferreira, and J. Oliveira, "Hardware-efficient chromatic dispersion estimator based on parallel Gardner timing error detector," presented at the Optical Fiber Communication Conf., Anaheim, CA, USA, Mar. 17–21, 2013, Paper OTh3C.6.
[8] R. Borkowski, X. Zhang, D. Zibar, R. Younce, and I. T. Monroy, "Experimental demonstration of adaptive digital monitoring and compensation of chromatic dispersion for coherent DP-QPSK receiver," *Opt. Exp.*, vol. 19, no. 26, pp. B728–B735, Dec. 2011.
[9] C. Malouin, P. Thomas, B. Zhang, J. O'Neil, and T. Schmidt, "Natural expression of the best-match search Godard clock-tone algorithm for blind chromatic dispersion estimation in digital coherent receivers," presented at the Signal Processing Photonic Communications, Colorado Springs, CO, USA, Jun. 19–21, 2012, Paper SpTh2B.4.
[10] C. Malouin, M. Arabaci, P. Thomas, B. Zhang, T. Schmidt, and R. Marcoccia, "Efficient, non-data-aided chromatic dispersion estimation via generalized, FFT-based sweep," presented at the Optical Fiber Communication Conf., Anaheim, CA, USA, Mar. 17–21, 2013, Paper JW2A.45.
[11] Q. Sui, A. P. T. Lau, and C. Lu, "Fast and robust chromatic dispersion estimation using auto-correlation of signal power waveform for DSP based-coherent systems," presented at the Optical Fiber Communication Conf., Los Angeles, CA, USA, Mar. 4–8, 2012, OW4G.3.
[12] Q. Sui, A. P. T. Lau, and C. Lu, "Fast and robust blind chromatic dispersion estimation using auto-correlation of signal power waveform for digital coherent systems," *J. Lightw. Technol.*, vol. 31, no. 2, pp. 306–312, Jan. 2013.
[13] F. C. Pereira, V. N. Rozental, and D. A. A. Mello, "Limitations of the power auto-correlation-based chromatic dispersion estimation method in dispersion-managed links," presented at the Latin America Optics Photonics Conf., Sao Sebastiao, Brazil, Nov. 10–13, 2012, Paper LM4C.4.
[14] J. Proakis, *Digital Signal Processing: Principles, Algorithms, and Applications,* 3rd ed. Englewood Cliffs, NJ, USA: Prentice-Hall, 1996.
[15] A. Oppenheim, R. Schafer, and J. Buck, *Discrete-Time Signal Processing,* 2nd ed. Englewood Cliffs, NJ, USA: Prentice-Hall, 1999.
[16] ITU-T Recommendation G.709: Interfaces for the Optical Transport Network, 2012. [Online]. Available: http://www.itu.int/rec/T-REC-G.709-201202-I/en